A new laser peening technique: femtosecond laser peening without a sacrificial overlay under atmospheric conditions

Tomokazu Sano
Osaka University, Japan, sano@mapse.eng.osaka-u.ac.jp

Keywords: laser peening, femtosecond laser, fatigue properties, residual stress, hardness

Introduction

Laser peening, or laser shock peening, is a surface modification technology using laser-driven shock compression to improve the properties of metals such as hardness, residual stress, fatigue properties, and corrosion resistance [1-4]. A nanosecond pulsed laser is presently utilized as a laser peening tool in aerospace, automotive, medical, and nuclear industries [4]. The solid material which is irradiated by a nanosecond laser pulse transforms into gas or plasma via a liquid, accompanied by a volume expansion. A shock wave is driven as a recoil force during the expansion on the surface and propagates into the material [5,6]. The plastic deformation of the material via the shock wave contributes to the peening effect [7]. In the case where a laser pulse with a near infrared wavelength (~ 1.05 μm) is used, the material's surface needs to be covered with a protective coating or a sacrificial layer such as a black paint or an aluminum tape to prevent the surface from melting or sustaining damage from the laser pulse [4,8]. After the laser treatment, the remaining coating needs to be removed. Laser peening without coating process was developed using 532 nm wavelength lasers by optimizing process conditions, which has been applied to practical uses in nuclear industries [3]. However, the surface needs to be covered with a transparent medium such as water to suppress the plasma expansion and obtain a high amplitude of the shock wave sufficient to deform the material plastically for both wavelengths. Although a micro laser shock peening process has been developed using the shorter wavelength of 355 nm with tens of nanosecond pulse width to suppress thermal damage, this process also requires both a coating and water [9]. The nanosecond laser process does not produce a sufficient shock wave without covering the surface with a plasma confinement medium. Although the applicability of laser peening will clearly be increased if a plasma confinement medium is not required, such a technique has never been realized for the nanosecond laser process.

The intensity of a femtosecond laser pulse, which is equivalent to the energy per unit time and unit area and is proportional to the square of the electric field intensity, is extremely high even at a low energy because the pulse width is extremely short [10]. Therefore, direct irradiation of a solid surface with a femtosecond laser pulse drives an intense shock wave that propagates into the solid [11]. Such a shock wave driven by the femtosecond laser pulse irradiated under atmospheric conditions deforms a material plastically, resulting in quenching metastable high-pressure phases [12,13] or forming a high density of dislocations [14-17] Heat-affected and melted zones formed by a femtosecond laser pulse are much smaller than those produced by a nanosecond laser pulse due to its extremely short pulse width [18,19]. Therefore, peening without a sacrificial overlay under atmospheric conditions is considered to be possible using a femtosecond laser pulse. Femtosecond laser peening of steel under water [20,21] and femtosecond laser peen forming of thin metal sheet in the air [22,23] have been reported. However, femtosecond laser peening without a sacrificial overlay under atmospheric conditions aiming to improve mechanical properties has never been reported.

Objectives

The purpose of this study is to investigate the possibility of the femtosecond laser peening without a sacrificial overlay under atmospheric conditions. The material used in this study was a precipitation-hardened 2024 aluminum alloy which is commercially used in the aerospace industry. The surface morphology and microstructure were observed and its mechanical properties such as hardness, residual stress, and fatigue properties were measured to evaluate the peening effects.

Methodology

A 2024-T351 aluminum alloy was used in this study except for the fatigue tests, where a 2024-T3 aluminum alloy was used. Table 1 shows the chemical composition in mass% of these aluminum alloys. The proof stress of 2024-T351 and 2024-T3 alloys are 321 MPa and 334 MPa, respectively. The surface of the specimen to be irradiated by laser pulses was electropolished in 20% sulfuric acid-methanol electrolyte for 30 s to remove the work-strained layer.

Figure 1 schematically illustrates the experimental setup for femtosecond laser peening. The specimen of 2024-T351 aluminum alloy specimen with the dimensions of 10 x 10 x 10 mm^3 was mounted on an *x*-*y* stage as shown in Fig. 1(a). Femtosecond laser pulses (Spectra-Physics Inc., Spitfire) with a wavelength of 800 nm and a pulse width of 120 fs were focused using a plano-convex lens with a focal length of 70 mm and irradiated normal to the electropolished surface of the specimen in the air. Before the peening experiment, the depth etched by a single pulse of femtosecond laser was investigated as a function of pulse energy to select the peening conditions. The crater depth formed by femtosecond laser irradiation at a fixed position was measured using a laser microscope. The removed depth per pulse was estimated by dividing the crater depth by the number of irradiation pulses.

For the peening treatment, the aluminum specimen was moved in the *x*- and *y*- directions during laser irradiation as shown in Fig. 1(b). A coverage C_v, which is expressed by $C_v = \pi D^2 N_p / 4$ where D is the spot diameter of the laser pulse irradiated and N_p is the number of pulses per unit square. N_p is varied by changing the moving speed in the *x*-direction and the pulse-to-pulse distance in the *y*-direction. Based on the relationship between the removed depth and the pulse energy, five pulse energies of 5, 30, 75, 200, and 600 μJ, which corresponded to spot diameters of 12, 30, 40, 60, and 70 μm, respectively, and two different coverages of 692% and 2768% were chosen for peening treatment.

Surface morphology was observed using a scanning electron microscope (SEM, HITACHI S-3000H). Microstructure was observed using a transmission electron microscope (TEM, JEOL JEM-2010). For TEM observations, a small piece of the cross section was thinned by a 30 keV focused Ga-ion beam (HITACHI FB-2000). The residual stress on the laser-irradiated surface was measured from the Al(222) diffraction peak of CrKα X-rays (2.2897 Å) using a stress constant of -96.89 MPa/degree, which was calculated using the Kröner model [24] with a single-crystal elastic stiffness (C_{11} = 106.78 GPa, C_{12} = 60.74 GPa, and C_{44} = 28.21 GPa) [25]. Thin layers of the surface were successively removed by electrolytic polishing to obtain the depth profile of the residual stress. The hardness of the cross section was measured using a nanoindentation system (ELIONIX ENT-1100a) with the applied load of 1 mN. Before the nanoindentation test, the cross section was polished by a 5 keV Ar-ion beam (JEOL SM-09010) to remove the work-hardened layer.

The shape and dimensions of the fatigue specimens of the 2024-T3 aluminum alloy are shown in Fig. 1(c). The

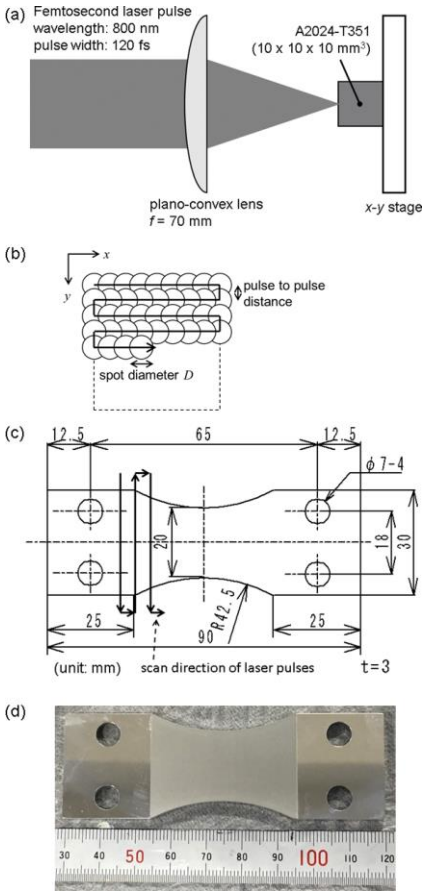

Fig. 1 Schematic illustrations of (a) the experimental setup for laser irradiation, (b) the scan direction of laser pulses for the setup shown in (a), and (c) shape and dimensions of fatigue test specimens and scan direction of laser pulses for fatigue specimens. Picture of fatigue test specimen corresponding to (c) is shown in (d).

thickness of the specimen was 3 mm. Both top and bottom surfaces were mirror-finished in the same manner as the 2024-T351 specimens. Femtosecond laser peening treatments were performed for both surfaces. Picture of fatigue test specimen after the femtosecond laser peening treatment is shown in Fig. 1(d). Plane bending tests were conducted at a cyclic speed of 1400 cycles/min with a constant strain amplitude and a stress ratio of R = -1 in the air at room temperature.

Table 1. Chemical composition in mass% of 2024-T351 and 2024-T3 aluminum alloys used in this study.

	Si	Fe	Cu	Mn	Mg	Cr	Zn	Ti	Others	Al
2024-T351	0.08	0.10	4.6	0.53	1.5	0.00	0.03	0.02	0.04	Bal.
2024-T3	0.02	0.05	4.4	0.55	1.4	0.00	0.02	0.01	0.01	Bal.

Results and analysis

The relationships between the removed depth per pulse and the pulse energy is shown in Fig. 2. The gradient above 30 μJ is larger than that below 30 μJ, suggesting that a stronger shock pressure is driven above 30 μJ because the larger volume of the removed material creates a larger recoil force. Therefore, pulse energies of 5, 30, 75, 200 and 600 μJ, which are below, at, and above 30 μJ, were chosen for the peening experiments to confirm the existence of the threshold.

Figure 3 shows the SEM images of the laser-irradiated surface for the pulse energies of 30, 75, and 600 μJ and coverages of 692 and 2768 %. Regardless of the condition, droplets are not observed, indicating that the femtosecond laser treatment creates a negligibly small molten layer.

The results of the residual stress measurements for surfaces of the femtosecond laser irradiated material with coverage of 692% and 2768% are shown in Fig. 4. Compressive residual stress is achieved above 30 μJ, which corresponds to the point where the gradient of the removed depth per pulse energy changes. This means that a pulse energy above 30 μJ sufficiently drives a shock wave to induce plastic deformation. A larger pulse energy gives a larger compressive stress for a given coverage. The compressive stress for the coverage of 692% is slightly larger than that for the coverage of 2768% for the same pulse energy. Here, σ_x is larger than σ_y below 30 μJ, but this tendency is reversed above 75 μJ for given coverages. The depth profiling results of σ_x for 600 μJ and 2768% are shown in Fig. 4(c). The maximum compressive residual stress around 300 MPa is attained at a depth of 4 μm from the surface. This value is almost equal to the 0.2% proof stress of 2024-T351 aluminum alloy26 and the values obtained using other peening methods such as nanosecond laser peening, shot peening, or ultrasonic peening [27-32]. The compressive stress decreases to zero around 90 μm, which is around one tenth of the peened depth obtained by nanosecond laser peening.

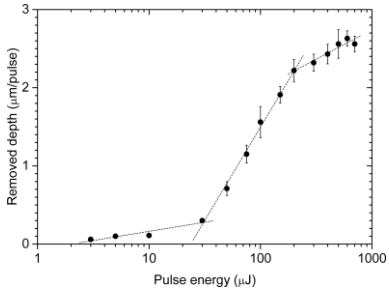

Fig. 2. Relationships between the removed depth per pulse and the pulse energy.

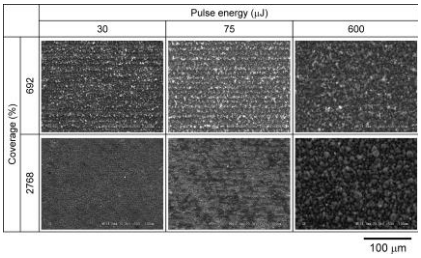

Fig. 3. SEM images of the surface of 2024-T351 specimen after femtosecond laser peening.

The results of hardness measurements in the cross section of the laser irradiated specimen are shown in Fig. 5. The data in the hardened region are fit by polynomial curves. The maximum value of the curve is defined as the maximum hardness H_{max}, of which corresponding depth is defined as the depth at the maximum hardness. The depth where the fitting curve matches the original hardness, which corresponds to the hardness at the depth of 40 μm, is defined as the hardened depth as well as the difference between the hardened depth and the depth at the maximum hardness as the thickness of the

hardened region (Table 2). Most of the surface region has a hardness similar to the original material, which corresponds to the SEM observation shown in Fig. 3 where most the surface region consists of debris. The maximum hardness is almost the same for each condition. A larger pulse energy forms a thicker hardened region for a given coverage. For the pulse energy of 600 μJ, the thickness of the hardened region with a 692% coverage is larger than that with a 2768 % coverage. A larger coverage induces more removed depth as well as increasing the thickness of the plastic deformed region. Therefore, a larger coverage does not necessarily form a thicker residual hardened region.

Table 2. Maximum hardness, depth at the maximum hardness, hardened depth, and thickness of the hardened region for each laser condition.

Laser conditions Pulse energy and coverage	Max. hardness (GPa)	Depth at max. hardness (μm)	Hardened depth (μm)	Thickness of hardened region (μm)
30 μJ and 692%	2.2	4.4	14.3	9.9
75 μJ and 692%	2.1	8.0	16.9	8.9
600 μJ and 692%	2.2	10.2	35.2	25.2
600 μJ and 2768%	2.3	11.1	28.0	16.9

Both surfaces of the fatigue test specimen shown in Fig. 1(c) were peened using a pulse energy of 600 μJ and a coverage of 2768%. The relationship between stress amplitude and number of cycles to failure of femtosecond laser-peened 2024-T3 aluminum alloy and base material is shown in Fig. 6. The fatigue life was improved as much as 38 times in comparison with base material at stress amplitude of 195 MPa. The fatigue strength at $2x10^6$ cycles of the peened specimen was 58 MPa larger than that of the base material. Fracture surfaces of a femtosecond laser peened specimen at a stress amplitudes of 280 MPa and 195 MPa are shown in Fig. 7. Cracks initiated from the surface for a stress amplitude of 280 MPa. For a stress amplitude of 195 MPa, crack initiation sites were located around 160 μm deep from the surface. For the lower stress amplitude, it is suggested that crack initiation from the surface was suppressed because the surface layer with a thickness of 28 μm was hardened and 90 μm was compressive, resulting in the internal crack initiation.

Figure 8 shows the TEM image of the cross section of 2024-T351 aluminum alloy irradiated by a pulse energy of 600 μJ with a coverage of 2768%. The surface is covered with a layer around 5 μm thick containing some voids, as shown in Fig. 8(a). These voids would cause the lack of a hardness increase in the surface region over a thickness of several

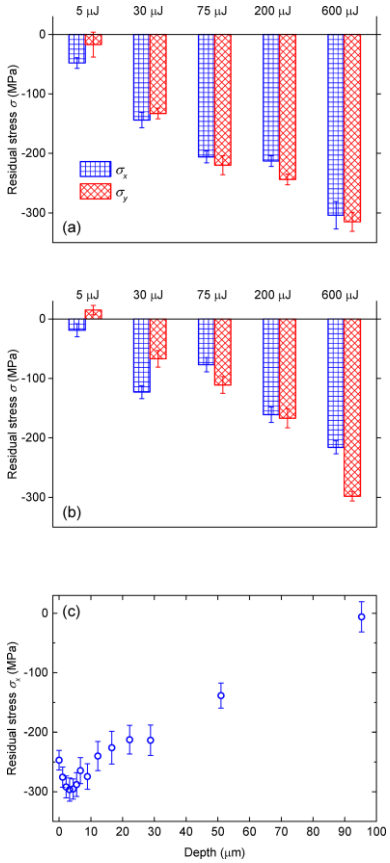

Fig. 4. Residual stress of the surface after femtosecond laser irradiation with a coverage of (a) 692% and (b) 2768%. Depth profile of the residual stress for the specimen irradiated with a pulse energy of 600 μJ and a coverage of 2768%. Error bars indicate measurement uncertainty.

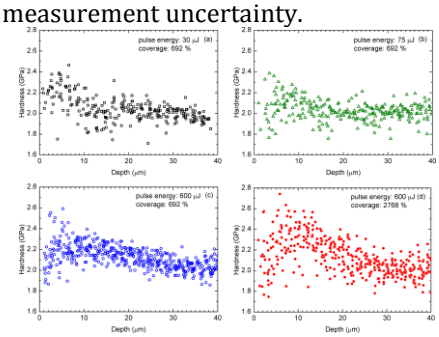

Fig. 5. Depth profile of the hardness in depth for the specimen irradiated by femtosecond laser pulses with (a) a pulse energy of 30 μJ and a coverage of 692%, (b) a pulse energy of 75 μJ and a coverage of 692%, (c) a pulse energy of 600 μJ and a coverage of 692%, and (d) a pulse energy of 600 μJ and a coverage of 2768%.

microns seen in Fig. 5. The magnified view of the interface between the surface layer and the lower solid material is shown in Fig. 8(b). A clear grain boundary exists at the interface, suggesting that the surface layer was formed after melting and resolidification.

As shown in Fig. 4(c), the residual stress in the top surface was compressive, even though the residual stress in a resolidified layer is generally tensile. As shown in Fig. 7(b), cracks did not initiate from voids in the resolidified layer for a lower stress amplitude, resulting in improved fatigue life at high cycles. A high density of dislocations exist in the upper resolidified layer as well as the solid material, indicating both layers were plastically deformed or peened by femtosecond laser-driven shocks. A shock front which is driven by a femtosecond laser pulse overtakes the heat front induced by the laser pulse, and finally forms a high density of dislocations in a region deeper than the heat affected zone [12,14,15]. Under the femtosecond laser peening condition for a coverage of 2768%, the shock front passes through about 2 nm thick molten layer and propagates into the resolidified layer which is formed by former laser pulses and the solid layer, resulting in providing peening effects on the material.

Conclusions

The fatigue properties of 2024 aluminum alloy were improved by femtosecond laser peening treated in the air without a sacrificial overlay such as a protective coating and water as a plasma confinement medium. With a pulse energy of 600 μJ and a coverage of 2768%, the fatigue life was improved as much as 38 times in comparison with base material at a stress amplitude of 195 MPa. The fatigue strength at $2x10^6$ cycles of the peened specimen was 58 MPa larger than that of the base material. For a stress amplitude of 195 MPa, crack initiation sites was located around 160 μm deep from the surface. The surface region was hardened over a depth of several tens of micrometers. The compressive residual stress induced in the surface region was almost equal to the 0.2% proof stress of 2024 aluminum alloy. The thickness of the layer with the compressive residual stress was around 100 μm. The femtosecond laser peening process has a great potential to be applied in various fields where conventional peening methods cannot be used, as this process can be performed under ambient conditions without the use of a plasma confinement medium such as water or transparent materials. For example, a micro device such as Nano- or Micro- Electro Mechanical Systems can be peened by femtosecond laser pulses because the range of the heat-affected zone by the pulses is on the nano- to micrometer

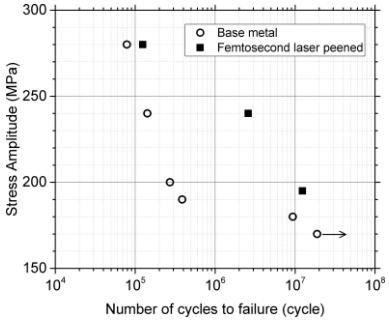

Fig. 6. Results of plane bending fatigue tests for specimens of femtosecond laser-peened 2024-T3 aluminum alloy and base material.

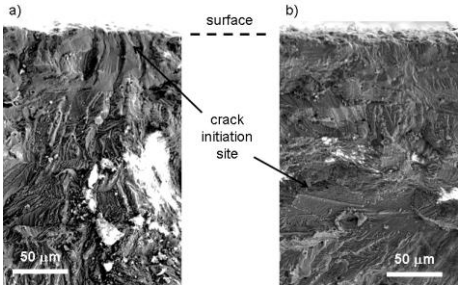

Fig. 7. Fracture surfaces of femtosecond laser-peened 2024-T3 aluminum alloy at stress amplitude of (a) 280 MPa and (b) 195 MPa.

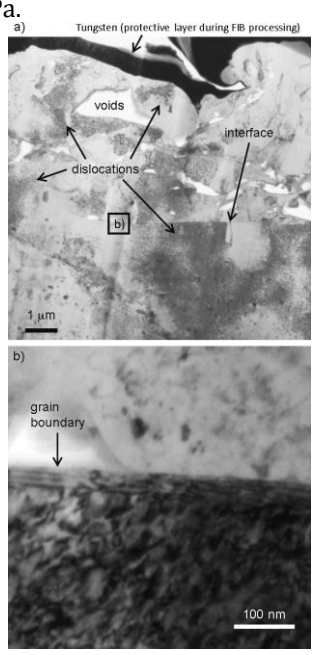

Fig. 8. (a) TEM image of the cross section of the femtosecond laser-irradiated 2024-T351 aluminum alloy with a pulse energy of 600 μJ and a coverage of 2768%. (b) Magnified view around the interface between the surface layer and the solid material.

scale. Additionally, this process can be theoretically performed in a vacuum because there is no significant difference of the shock pressure between driven in a vacuum and in the air, allowing this method to be used in space [33].

References

[1] A. H. Clauer, J. H. Holbrook, and B. P. Fairand, Shock Waves and High-Strain-Rate Phenomena in Metals, Plenum Publishing Corporation, New York 675-703 (1981).
[2] R. Fabbro, P. Peyre, L. Berthe, and X. Scherpereel, J. Laser Appl. 10, 265 (1998).
[3] Y. Sano, M. Obata, T. Kubo, N. Mukai, M. Yoda, K. Masaki, and Y. Ochi, Mater. Sci. Eng. A 417, 334 (2006).
[4] R. D. Tenaglia and D. F. Lahrman, "Shock tactics," Nat. Photonics 3, 267 (2009).
[5] P. Fairand and A. H. Clauer, J. Appl. Phys. 50, 1497 (1979).
[6] R. Fabbro, J. Fournier, P. Ballard, D. Devaux, and J. Virmont, J. Appl. Phys. 68, 775 (1990).
[7] P. Fairand, B. A. Wilcox, W. J. Gallagher, and D. N. Williams, J. Appl. Phys. 43, 3893 (1972).
[8] Y. Liao, C. Ye, and G. J. Cheng, Opt. Laser. Technol. 78, 15 (2016).
[9] W. Zhang, Y.L. Yao, and I. C. Noyan, ASME J. Manuf. Sci. Eng. 126, 10 (2004).
[10] D. Strickland and G. Mourou, Opt. Commun. 56, 219 (1985).
[11] R. Evans, A. D. Badger, F. Falliès, M. Mahdieh, T. A. Hall, P. Audebert, J.-P. Geindre, J.-C. Gauthier, A. Mysyrowicz, G. Grillon, and A. Antonetti, Phys. Rev. Lett. 77, 3359 (1996).
[12] T. Sano, H. Mori, E. Ohmura, and I. Miyamoto, Appl. Phys. Lett. 83, 3498 (2003).
[13] M. Tsujino, T. Sano, O. Sakata, N. Ozaki, S. Kimura, S. Takeda, M. Okoshi, N. Inoue, R. Kodama, K. F. Kobayashi, and A. Hirose, J. Appl. Phys. 110, 126103 (2011).
[14] M. Tsujino, T. Sano, T. Ogura, M. Okoshi, N. Inoue, N. Ozaki, R. Kodama, K. F. Kobayashi, and A. Hirose, Appl. Phys. Express 5, 022703 (2012).
[15] T. Matsuda, T. Sano, K. Arakawa, and A. Hirose, Appl. Phys. Lett. 105, 021902 (2014).
[16] T. Matsuda, T. Sano, K. Arakawa, and A. Hirose, J. Appl. Phys. 116, 183506 (2014).
[17] T. Matsuda, T. Sano, K. Arakawa, O. Sakata, H. Tajiri, and A. Hirose, Appl. Phys. Express 7, 122704 (2014).
[18] B. N. Chichkov, C. Momma, S. Nolte, F. von Alvensleben, and A. Tunnermann, Appl. Phys. A 63, 109 (1996).
[19] R. Le Harzic, N. Huot, E. Audouard, C. Jonin, P. Laporte, S. Valette, A. Fraczkiewicz, and R. Fortunier, Appl. Phys. Lett. 80, 3886 (2002).
[20] H Nakano, S. Miyauti, N. Butani, T. Shibayanagi, M. Tsukamoto, and N. Abe, J. Laser Micro/Nanoeng. 4, 35 (2009).
[21] D. Lee and E. Kannatey-Asibu, Jr., J. Laser Appl. 23, 022004 (2011).
[22] Y. Sagisaka, M. Kamiya, M. Matsuda, and Y. Ohta, J Mater. Process. Tech. 210, 2304 (2010).
[23] Y. Sagisaka, K. Yamashita, W. Yanagihara, and H. Ueta, J Mater. Process. Tech. 219, 230 (2015).
[24] E. Kröner, Zeiteschrift Physik 151, 504 (1958).
[25] N. Kamm and G. A. Alers, J. Appl. Phys. 35, 327 (1964).
[26] Z. Horita, T. Fujinami, M. Nemoto, and T. G. Langdon, Metall. Mater. Trans. A 31A, 691 (2000).
[27] A. H. Clauer, C. T. Walters, S. C. Ford, Lasers in Materials Processing, American Society for Metals, Metals Park, Ohio, 7 (1983).
[28] C. A. Rodopoulos, J. S. Romero, S. A. Curtis, E.R. de los Rios, and P. Peyre, J. Mater. Eng. Perform. 12, 414 (2003).
[29] C. A. Rodopoulos, S. A. Curtis, E. R. de los Rios, and J. SolisRomero, Int. J. Fatigue 26, 849 (2004).
[30] A. Ali, X. An, C. A. Rodopoulos, M. W. Brown, P. O'Hara, A. Levers, and S. Gardiner, Int. J. Fatigue 29, 1531 (2007).
[31] C. A. Rodopoulos, A. Th. Kermanidis, E. Statnikov, V. Vityazev, and O. Korolkov, J. Mater. Eng. Perform. 16, 30 (2007).
[32] A. Gariépy, F. Bridier, M. Hoseini, P. Bocher, C. Perron, and M. Lévesque, Surf. Coat. Tech. 219, 15 (2013).
[33] T. Sano, T. Eimura, R. Kashiwabara, T. Matsuda, Y. Isshiki, A. Hirose, S. Tsutsumi, K. Arakawa, T. Hashimoto, K. Masaki, and Y. Sano, J. Laser Appl. 29, 012005 (2017).